

## Metal Pillared Bentonite Synthesis and Its Characteristics Using X-Ray Diffraction

Sisnayati<sup>1</sup>, Muhammad Said<sup>2</sup>, Nabila Aprianti<sup>3</sup>, Ria Komala<sup>1</sup>,  
Hendra Dwipayana<sup>4</sup>, Muhammad Faizal<sup>3\*</sup>

<sup>1</sup> Chemical Engineering Department, Faculty of Engineering, Universitas Tamansiswa, Jl. Tamansiswa No. 261, 20 Ilir D. I, Ilir Tim. I, Kota Palembang, Sumatera Selatan, Indonesia

<sup>2</sup> Chemistry Department, Faculty of Mathematics and Natural Science, Universitas Sriwijaya, Jl. Raya Palembang-Prabumulih Km 32 Indralaya, Ogan Ilir, Sumatera Selatan 30662, Indonesia

<sup>3</sup> Chemical Engineering Department, Faculty of Engineering, Universitas Sriwijaya, Jl. Raya Palembang-Prabumulih Km 32 Indralaya, Ogan Ilir, Sumatera Selatan 30662, Indonesia

<sup>4</sup> Mechanical Engineering Department, Faculty of Engineering, Universitas Tamansiswa, Jl. Tamansiswa No. 261, 20 Ilir D. I, Ilir Tim. I, Kota Palembang, Sumatera Selatan, Indonesia

\* Corresponding author's e-mail: muhammadfaizal@unsri.ac.id

### ABSTRACT

Modification of bentonite by the Al/Fe metal oxide pillarization process was carried out with metal oxides. The bentonite pillars were successfully characterized using an X-Ray Diffraction (XRD) spectrophotometer. The results of XRD characterization showed the peak diffraction angle ( $2\theta$ ) in metal-pillared bentonite was  $26.84^\circ$  at 698.98 cps. Meanwhile, in thermally and chemically activated bentonite, the peak angles were marked at  $20.64^\circ$  and  $26.7^\circ$ . There is a shift in the peak angle after activation and pillarization. XRD patterns showed dioctahedral smectite and quartz accessory minerals.

**Keywords:** crystal structure, natural bentonite, pillared, Al/Fe.

### INTRODUCTION

Natural bentonite is a lamellar aluminosilicate mesoporous material with a crystal structure in which the interlayer space in the structure is occupied by replaceable cations, for example,  $\text{Na}^+$ ,  $\text{K}^+$ , and  $\text{Ca}^{+2}$  (Elfadly et al., 2017). Bentonite contains varying amounts of silica with montmorillonite as the base mineral and other minerals, such as quartz, calcite, and feldspar. The characteristics of bentonite depend on the amount of smectite. The properties of smectite, namely cation exchange capacity, particle size, pore structure, adsorption properties, surface area and catalytic activity, are strongly influenced by thermal treatment (Andrini et al., 2017). Bentonite from smectite, especially montmorillonite (80–90 wt%),

can expand several times its original volume when they come into contact with water, (Kumar and Lingfa, 2020). Calcium bentonite proved to be a catalyst for the pyrolysis of plastics (Panda, 2018). Although the crystal structure is different, the chemical composition of clay, feldspar and zeolite minerals are close (Özgüven et al., 2019).

Bentonite, a natural clay mineral with a layered structure, contains exchangeable inorganic cations (Andrunik and Bajda, 2019). The cations that can be exchanged, found in the structure of the bentonite layer, in addition to having the ability to expand, are also widely found in Indonesia. This is why this material is suitable for applications as adsorbents and catalysts (Goodarzi et al., 2016). However, bentonite has one drawback: a small distance between layers and unreliable

porosity. Modified clays can be divided into pillared layered clays, organoclays, nanocomposites, acid and salt-induced, and thermally and mechanically-induced modified clays (Motawie et al., 2014). Pillarization involves the insertion of ions, molecules or compounds in the bentonite interlayer (Wijaya et al., 2021). In this work, Al/Fe macro-anions were used as the insertion material. In addition to being in the bentonite, thus making the distance between the layers farther apart, metal oxides are also on the surface of the bentonite. This research aims to synthesize natural metal pillared bentonite and compare its characteristics with bentonite, which is activated by heating and chemical.

## MATERIALS AND METHOD

### Materials

The bentonite used in this study was categorized as natural bentonite purchased from Loba Chemie Pvt Ltd. The chemicals used to synthesize metal pillared bentonite consisted of  $\text{H}_2\text{SO}_4$ ,  $\text{Al}(\text{NO}_3)_3 \cdot 9\text{H}_2\text{O}$ ,  $\text{Fe}(\text{NO}_3)_3 \cdot 9\text{H}_2\text{O}$ , NaOH, and aquades ( $\text{H}_2\text{O}$ ).

### Purification and activation of natural bentonite through chemical process

The bentonite was cleaned and weighed 5 g, placed into a 250 mL beaker, added 200 mL of 5%  $\text{H}_2\text{SO}_4$ , and stirred using a magnetic stirrer for 8 h at room temperature. Then, the mixture was separated using centrifugation and washed with distilled water several times to remove the remaining  $\text{SO}_4^{2-}$  anions. The bentonite solid was dried in an oven at 80 °C for 8 h.

### Bentonite activation by thermal process

Natural bentonite is activated by calcination at a temperature range of dehydroxylation. Catalyst preparation was carried out by activating heating using a muffle furnace at a temperature of 400 °C with a heating rate of 5 °C/min for 3 hours calculated after the desired temperature was reached.

### Preparation of Al/Fe pillar solution

Al/OH polyhydroxy pillaring solution was prepared by adding 80 mL of 0.5M  $\text{Al}(\text{NO}_3)_3 \cdot 9\text{H}_2\text{O}$  into a 240 mL 0.5 M NaOH solution mixed in a

500 mL beaker. The Fe/OH pillar solution was prepared by adding 40 mL of 0.5 M  $\text{Fe}(\text{NO}_3)_3 \cdot 9\text{H}_2\text{O}$  mixed in a 500 mL beaker into 240 mL of 0.5 M NaOH solution. The Al/Fe pillar solution mixture was stirred for 2 h and then allowed to stand for 2 days at room temperature.

## Characterization

The structural changes were analyzed using the X-Ray diffraction (XRD) method using the Rigaku Miniflex 600 X-Ray diffractometer with CuK radiation at 30 kV and 10 mA. The analysis was carried out at a scanning speed of 10 °/min at  $2\theta$  with a range of 5–80°.

## RESULTS AND DISCUSSION

### Materials characteristics

#### Aluminum nitrate [ $\text{Al}(\text{NO}_3)_3$ ]

The XRD pattern of  $\text{Al}(\text{NO}_3)_3$  is presented in Figure 1. The sharp peak characteristic of  $\text{Al}(\text{NO}_3)_3$  is seen at the diffraction angles of 22.70°, 30.14°, 39.34°, 52.20°, 73.60° and 83.44°. From Figure 1, it can be observed that the diffraction angle is  $2\theta$  22.70° with a peak intensity of 127.943 cps. At a diffraction angle of  $2\theta$  30.14°, the peak intensity is 4356.526 cps, and at a diffraction angle of  $2\theta$  52.20°, the peak intensity is 481.765 cps. The diffraction angle is a special characteristic of  $\text{Al}(\text{NO}_3)_3$  material which produces the distance between cells at the sharpest peak (30.14°) is 2.96 Å. This XRD pattern corresponds to the standard JCPDS file (card no. 24-0004), wherein the angle range of  $\text{Al}(\text{NO}_3)_3$  is  $\pm 22^\circ$ ,  $\pm 30^\circ$ ,  $\pm 39^\circ$ ,  $\pm 45^\circ$ ,  $\pm 52^\circ$ ,  $\pm 73^\circ$ ,  $\pm 83^\circ$ , corresponding to the (102), (110), (103), (200), (112), (004), (104) (Gabrovská et al., 2007).

#### XRD of $\text{Fe}(\text{NO}_3)_3$

The diffraction pattern of  $\text{Fe}(\text{NO}_3)_3$  is shown in Figure 2. The characteristic sharp peaks of  $\text{Fe}(\text{NO}_3)_3$  are seen at the diffraction angles of 20.28°, 54.66°, and 79.27°. At a diffraction angle of  $2\theta$  20.28°, the peak intensity is 376.805 cps, at a diffraction angle of  $2\theta$  54.66°, the peak intensity is 620.22 cps, and at a diffraction angle of  $2\theta$  79.27°, the peak intensity is 740.66 cps. The diffraction angle is a special characteristic of  $\text{Fe}(\text{NO}_3)_3$  material which produces the distance between cells at the sharpest peak (54.66°) is 2.8 Å. This XRD pattern

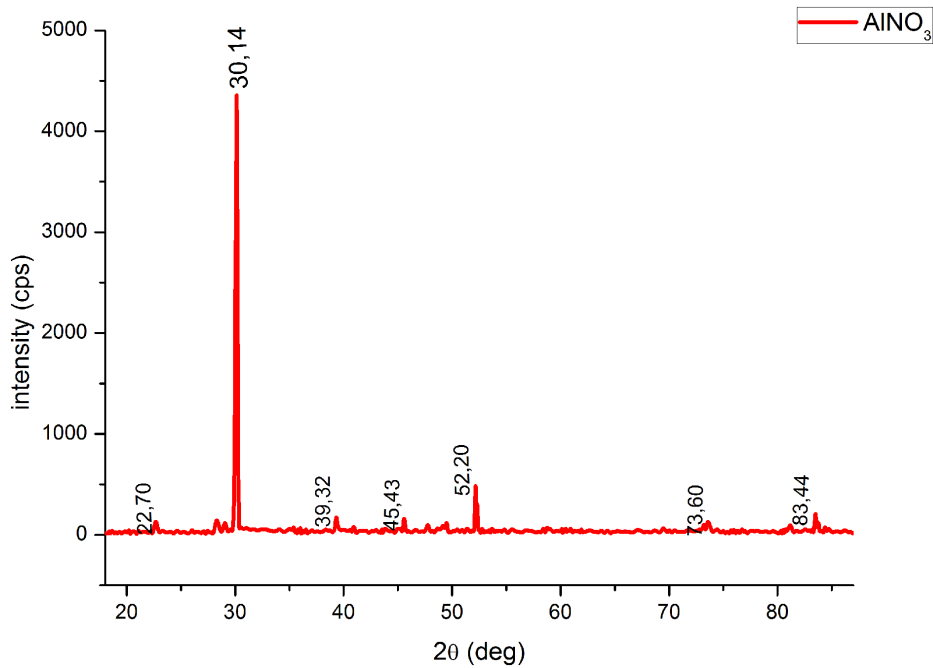


Figure 1. Diffractogram of Al(NO<sub>3</sub>)<sub>3</sub>

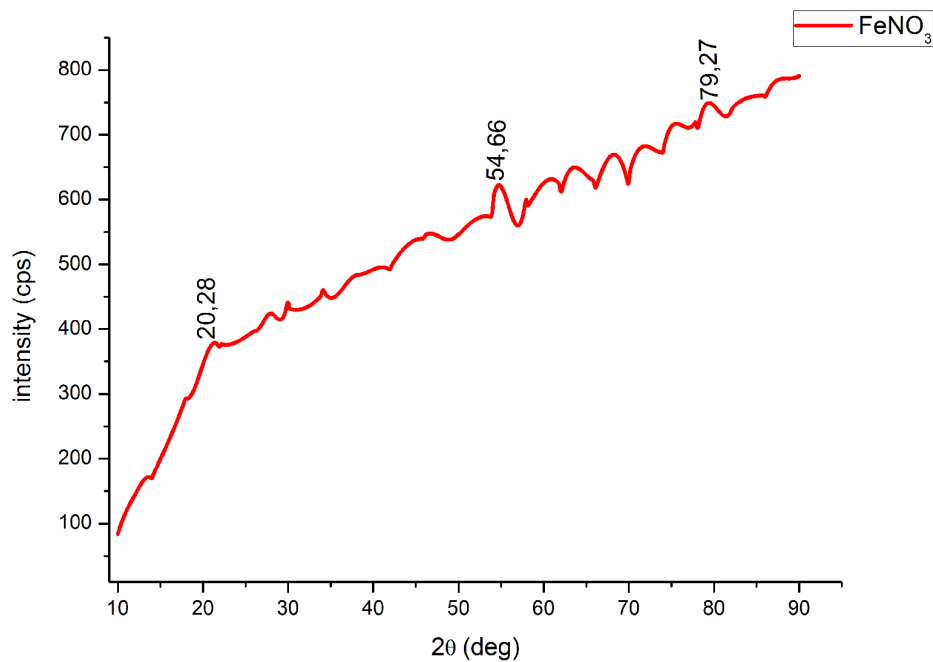


Figure 2. Diffractogram of Fe(NO<sub>3</sub>)<sub>3</sub>

corresponds to the standard JCPDS file (No. 19-0629), where the angle range of Fe(NO<sub>3</sub>)<sub>3</sub> starts from  $2\theta = \pm 20^\circ, \pm 26^\circ, \pm 55^\circ, \text{ and } \pm 79^\circ$  with planes (002), (042) and (151) (Dissanayake et al., 2020).

### Characteristics of natural bentonite

Figure 3 shows the diffraction pattern of natural bentonite. Sharp peaks of natural bentonite are

seen at diffraction angles of  $20.28^\circ$  and  $26.76^\circ$ . The diffraction angle is observed at  $2\theta 20.28^\circ$  with peak intensity of 555.891 cps, and at a diffraction angle of  $2\theta 26.76^\circ$ , the peak intensity is 858.903 cps. The diffraction angle is a special characteristic of bentonite material which shows the presence of anions between the natural bentonite layers and results in the distance between cells at the sharpest peak ( $26.76^\circ$ ) 4.26 Å. The initial XRD

pattern shows dioctahedral smectite and easily distinguishable accessory minerals of quartz and K-feldspar (Pentrák et al., 2018).

### Characteristics of thermal and chemical activated and Al/Fe pillared bentonite samples

The peak position values of natural bentonite and metal pillared bentonite samples were analyzed from the standard peak position values associated with the Joint Committee for Powder Diffraction Standards (JCPDS).

### Characteristics of thermal activated natural bentonite

Thermally activated bentonite was characterized using XRD. The diffraction pattern is shown in Figure 4. The sharp peak characteristic of pure bentonite is seen at the diffraction angles of  $20.64^\circ$  and  $26.68^\circ$ . In the diffractogram, the diffraction angle of  $2\theta$   $20.64^\circ$  shows a peak intensity of 484.69 cps, and at a diffraction angle of  $2\theta$   $26.68^\circ$ , it offers a peak intensity of 777.77 cps. The diffraction angle is a special characteristic of

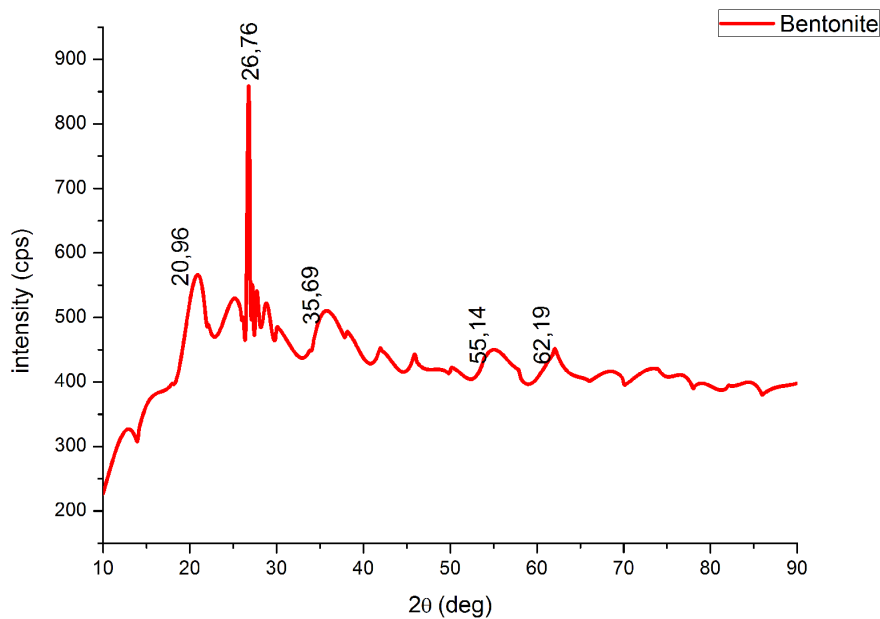


Figure 3. Diffractogram of natural bentonite

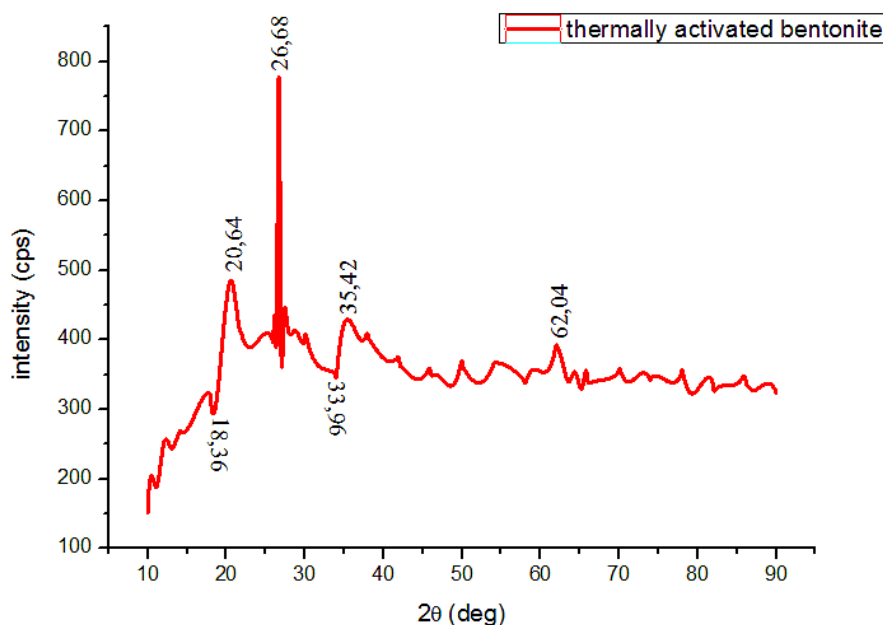


Figure 4. Thermal activated natural bentonite diffractogram

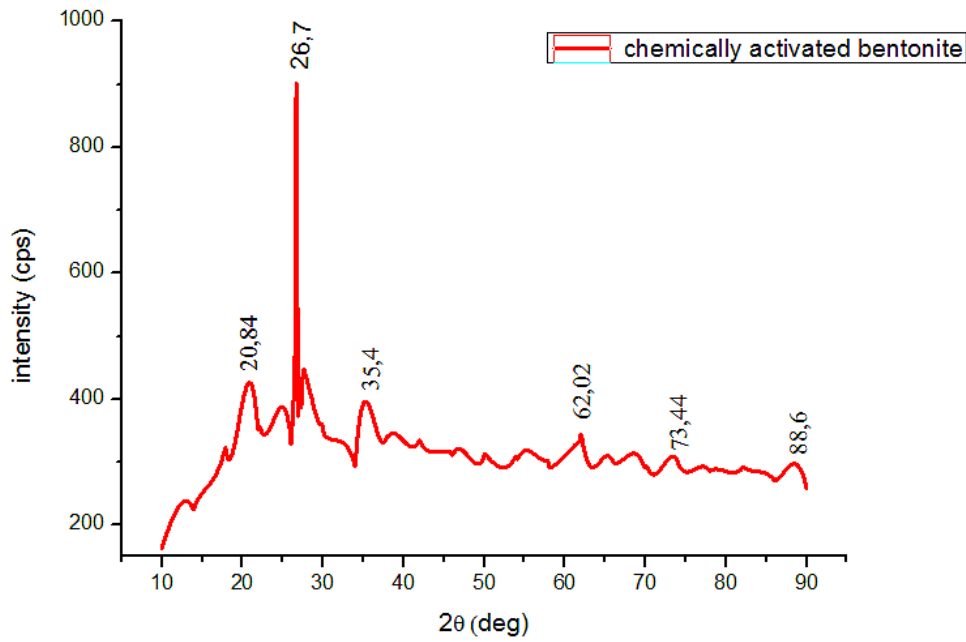


Figure 5. Diffractogram of chemical activated natural bentonite

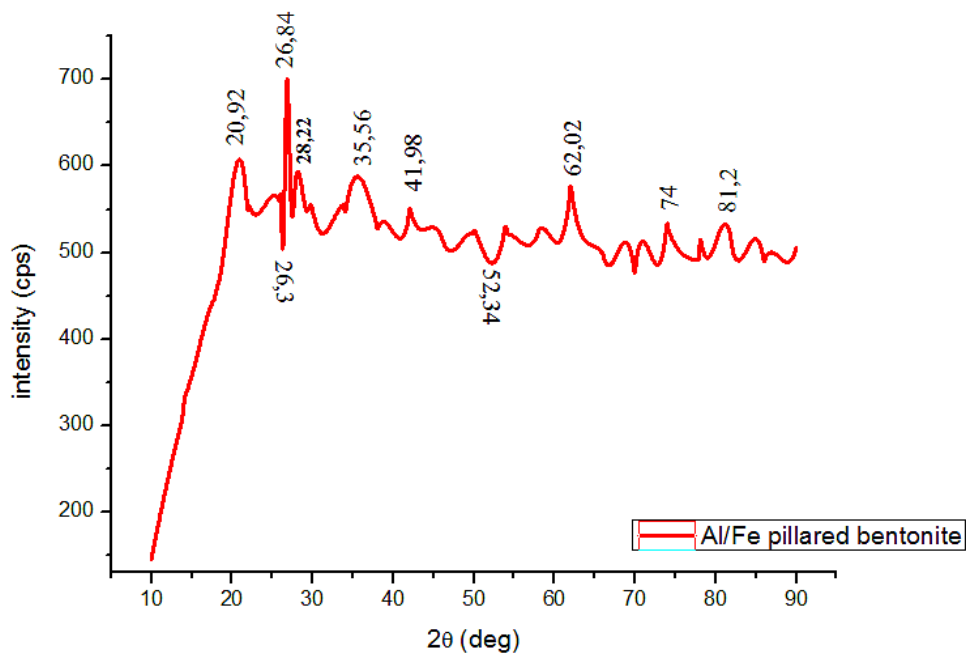


Figure 6. Al/Fe pillared natural bentonite diffractogram

bentonite material which shows the presence of anions between the natural bentonite layers and produces the distance between cells at the sharpest peak (26.68°).

### Characteristics of chemical activated bentonite

Chemically activated bentonite was characterized using XRD. The diffraction pattern is

shown in Figure 5. The sharp peak characteristic of pure bentonite is seen at the diffraction angles of 20.84° and 26.7°. At a diffraction angle of 2θ 20.84°, the peak intensity is 425.93 cps; at a diffraction angle of 2θ 26.7°, the peak intensity is 901.69 cps. The diffraction angle is a special characteristic of bentonite material which shows the presence of anions present between the natural bentonite layers and produces the distance between cells at the sharpest peak (26.7°).

## Characteristics of Al/Fe pillared bentonite

Natural and chemical-modified bentonite is used directly or as an industrial feedstock in many areas, depending on its physicochemical properties (Hasanudin et al., 2022; Kar et al., 2019; Komadel, 2016). Al/Fe-pillared bentonite was characterized using XRD, as shown in Figure 6. The sharp peaks characteristic of pure bentonite was seen at diffraction angles of  $20.92^\circ$ ,  $26.84^\circ$ , and  $35.56^\circ$ . The diffraction angle of  $2\theta$   $20.92^\circ$  shows a peak intensity of 606.803 cps. At a diffraction angle of  $2\theta$   $26.84^\circ$ , the peak intensity is 698.98 cps, and at a diffraction angle of  $2\theta$   $35.56^\circ$ , the peak intensity is 588 cps. The diffraction angle is a special characteristic of bentonite material which shows the presence of anions between the natural bentonite layers and produces the distance between cells at the sharpest peak ( $26.84^\circ$ ).

## CONCLUSIONS

The bentonite pillars were successfully characterized using an XRD spectrophotometer. The results of XRD characterization showed the peak diffraction angle ( $2\theta$ ) in metal-pillared bentonite was  $26.84^\circ$  at 698.98 cps. Meanwhile, in thermally and chemically activated bentonite, the peak angles were marked at  $20.64^\circ$  and  $26.7^\circ$ . The peak angle shifts after the bentonite is thermally, chemically activated, and polarized. Bentonite shows the presence of dioctahedral smectite and quartz minerals.

## Acknowledgments

This research was financially supported by Ministry of Education, Culture, Research, and Technology of the Republic of Indonesia through *Penelitian Dasar Kompetitif Nasional* scheme (Grant Number: 142/E5/PG.02.00.PT/2022 and 0148.011/UN9.3.1/PL/2022).

## REFERENCES

1. Andrini L., Moreira Toja R., Gauna M.R., Conconi M.S., Requejo F.G., Rendtorff N. M. 2017. Extended and local structural characterization of a natural and 800 °C fired Na-montmorillonite–Patagonian bentonite by XRD and Al/Si XANES. *Applied Clay Science*, 137, 233–240. <https://doi.org/10.1016/j.clay.2016.12.030>
2. Andrunik M., Bajda T. 2019. Modification of bentonite with cationic and nonionic surfactants: Structural and textural features. *Materials*, 12(22). <https://doi.org/10.3390/ma12223772>
3. Dissanayake D.M.S.N., Mantilaka M.M.M.G.P.G., Pitawala H.M.T.G.A. 2020. Synthesis of low-cost magnetite nano-architectures from Sri Lankan laterites. *Journal of Geological Society of Sri Lanka*, 21(2), 90–100.
4. Elfadly A.M., Zeid I.F., Yehia F.Z., Abouelela M.M., Rabie A.M. 2017. Production of aromatic hydrocarbons from catalytic pyrolysis of lignin over acid-activated bentonite clay. *Fuel Processing Technology*, 163, 1–7. <https://doi.org/10.1016/j.fuproc.2017.03.033>
5. Gabrovska M., Edreva-Kardjieva R., Angelov V., Crişan D., Munteanu G., Védrine J. 2007. Mg-Al and Mg-In oxide compounds as catalyst components for the oxidative dehydrogenation of propane. Part I - Preparation and characterization of the as-synthesized materials. *Revue Roumaine de Chimie*, 52(5), 521–525.
6. Goodarzi A.R., Najafi Fateh S., Shekary H. 2016. Impact of organic pollutants on the macro and microstructure responses of Na-bentonite. *Applied Clay Science*, 121–122, 17–28. <https://doi.org/10.1016/j.clay.2015.12.023>
7. Hasanudin H., Asri W.R., Zulaikha I.S., Ayu C., Rachmat A., Riyanti F., Hadiah F., Zainul R., Maryana R. 2022. Hydrocracking of crude palm oil to a biofuel using zirconium nitride and zirconium phosphide-modified bentonite. *RSC Advances*, 12(34), 21916–21925. <https://doi.org/10.1039/d2ra03941a>
8. Kar Y., Bozkurt G., Yalman Y. 2019. Liquid fuels from used transformer oil by catalytic cracking using bentonite catalyst. *Environmental Progress and Sustainable Energy*, 38(4), 1–6. <https://doi.org/10.1002/ep.13080>
9. Komadel P. 2016. Acid activated clays: Materials in continuous demand. *Applied Clay Science*, 131, 84–99. <https://doi.org/10.1016/j.clay.2016.05.001>
10. Kumar A., Lingfa P. 2020. Sodium bentonite and kaolin clays: Comparative study on their FT-IR, XRF, and XRD. *Materials Today: Proceedings*, 22, 737–742. <https://doi.org/10.1016/j.matpr.2019.10.037>
11. Motawie A.M., Madany M.M., El-Dakrory A.Z., Osman H.M., Ismail E.A., Badr M.M., El-Komy D. A., Abulyazied D.E. 2014. Physico-chemical characteristics of nano-organo bentonite prepared using different organo-modifiers. *Egyptian Journal of Petroleum*, 23(3), 331–338. <https://doi.org/10.1016/j.ejpe.2014.08.009>
12. Özgüven F.E., Pekdemir A.D., Önal M., Sarıkaya Y. 2019. Characterization of a bentonite and its permanent aqueous suspension. *Journal of the Turkish Chemical Society, Section A: Chemistry*, 7(1), 11–18. <https://doi.org/10.18596/jotcsa.535937>
13. Panda A.K. 2018. Thermo-catalytic degradation of different plastics to drop in liquid fuel using calcium

- bentonite catalyst. *International Journal of Industrial Chemistry*, 9(2), 167–176. <https://doi.org/10.1007/s40090-018-0147-2>
14. Pentrák M., Hronský V., Pálková H., Uhlík P., Komadel P., Madejová J. 2018. Alteration of fine fraction of bentonite from Kopernica (Slovakia) under acid treatment: A combined XRD, FTIR, MAS NMR and AES study. *Applied Clay Science*, 163(April), 204–213. <https://doi.org/10.1016/j.clay.2018.07.028>
15. Wijaya K., Kurniawan M.A., Saputri W.D., Trisunaryanti W., Mirzan M., Hariani P.L., Tikoalu A.D. 2021. Synthesis of nickel catalyst supported on ZrO<sub>2</sub>/SO<sub>4</sub> pillared bentonite and its application for conversion of coconut oil into gasoline via hydrocracking process. *Journal of Environmental Chemical Engineering*, 9(4), 105399. <https://doi.org/10.1016/j.jece.2021.105399>